

See discussions, stats, and author profiles for this publication at: <https://www.researchgate.net/publication/11513977>

Heteroatom Influence on the π -Facial Selectivity of Diels–Alder Cycloadditions to 1-Oxa-4-thia-6-vinylspiro[4.5]dec-6-ene, 3-Methoxy-3-methyl-2-vinylcyclohexene, and 3-Methoxy-2-vi...

ARTICLE *in* THE JOURNAL OF ORGANIC CHEMISTRY · MARCH 2002

Impact Factor: 4.72 · DOI: 10.1021/jo0106400 · Source: PubMed

CITATIONS

16

READS

32

5 AUTHORS, INCLUDING:



Veejendra Kumar Yadav

Indian Institute of Technology Kanpur

98 PUBLICATIONS 1,203 CITATIONS

SEE PROFILE

Heteroatom Influence on the π -Facial Selectivity of Diels–Alder Cycloadditions to 1-Oxa-4-thia-6-vinylspiro[4.5]dec-6-ene, 3-Methoxy-3-methyl-2-vinylcyclohexene, and 3-Methoxy-2-vinylcyclohexene^{†,‡}

Veejendra K. Yadav,^{*,§} Govindaraji Senthil,[§] K. Ganesh Babu,[§] Masood Parvez,^{||,⊥} and Jennifer Lee Reid^{||}

Department of Chemistry, Indian Institute of Technology, Kanpur 208 016, India, and Department of Chemistry, University of Calgary, Calgary, Alberta, Canada T2N 1N4

vijendra@iitk.ac.in

Received June 22, 2001

The facial selectivities of the Diels–Alder cycloadditions of several dienophiles to the title substrates were studied. The observed selectivities are interpreted as a consequence of the relative steric interactions offered by the substituents. The addition of dimethylacetylene dicarboxylate (DMAD) is influenced by the electrostatic repulsion arising from the interaction of an electron pair orbital on the acetal oxygen and the orthogonal π -orbital of the acetylene unit in DMAD in the *syn*-to-oxygen addition of the latter. This repulsion is offset on coordination of Li⁺ to the said oxygen electron pair orbital, and the addition thus proceeds *syn* to oxygen. The enhanced and accelerated *syn*-to-oxygen addition in lithium perchlorate in nitromethane is interpreted as a consequence of the coordination of Li⁺ to both the acetal oxygen and a heteroatom in the dienophile that brings them in close proximity to facilitate a reaction. The Li⁺–oxygen combination, however, also exerts some steric effect that results in reduced *syn*-to-oxygen addition of dienophiles having large substituents such as *N*-phenylmaleimide.

Introduction

The Diels–Alder (DA) cycloaddition is one of the standard methods for forming six-membered carbocycles as well as heterocycles.¹ The most recent stereochemical issue is that of π -facial control² that arises when a dienophile adds to the two faces of a diene at different rates. To enhance the required facial discrimination, a suitable understanding of the factors responsible for this differential reactivity becomes a genuine necessity. The factors known to influence the π -facial selectivity are (a) the presence of a chiral center in the diene or dienophile or both and (b) the presence of a chiral Lewis acid catalyst. The facial discrimination is achieved by effectively blocking one prochiral face of the substrate so that the addition takes place on the less hindered face to avoid steric destabilization. Other factors such as

π -orbital distortion,³ hyperconjugative interactions,⁴ secondary orbital interactions,⁵ torsional effects,⁶ electrostatic interactions,⁷ van der Waals–London attractions,⁸ polarizability effects,⁹ and product stability¹⁰ may also induce π -selectivity.

The directing effect of a heteroatom in DA cycloadditions has been extensively studied. From the work of Woodward on cycloadditions to 5-acetoxycyclopentadiene¹¹ and that of Fallis on the cycloadditions to 5-oxygen- and 5-sulfur-substituted pentamethylcyclopentadienes,¹² the addition is understood to occur *syn* to oxygen and *anti* to sulfur. When these *syn*- and *anti*-directing effects of oxygen and sulfur are coupled together, one is led to expect a highly enhanced *syn*-to-oxygen addition in reactions of dienes that have both O and S at the same carbon. These results, however, could not be extrapolated to **1** (Figure 1). There was no evidence for the *syn*-directing effect of the allylic oxygen on the additions of NPM and TCNE.¹³ Franck and co-workers¹⁴ have studied

* To whom correspondence should be addressed. FAX: 91-512-597436.

[†] This paper is dedicated to Professor H. Junjappa on the occasion of his 65th birthday.

[‡] Abbreviations: NMM = *N*-methylmaleimide, NPM = *N*-phenylmaleimide, MTAD = *N*-methyl-1,3,4-triazoline-2,5-dione, PTAD = *N*-phenyl-1,3,4-triazoline-2,5-dione, NQ = 1,4-naphthoquinone, DMAD = dimethylacetylene dicarboxylate, MVK = methyl vinyl ketone, PDC = pyridinium dichromate, EA = ethyl acrylate, TCNE = tetracyanoethylene, LPDE = lithium perchlorate in diethyl ether, LPNM = lithium perchlorate in nitromethane, TS = transition state, PPTS = pyridinium *p*-toluenesulfonate.

[§] Indian Institute of Technology.

^{||} University of Calgary.

[⊥] E-mail: parvez@acs.ucalgary.ca.

(1) Carruthers, W. *Some Modern Methods of Organic Synthesis*, 3rd ed.; Cambridge University Press: Cambridge, 1986; p 184. Oppolzer, W. In *Comprehensive Organic Synthesis*; Trost, B. M., Fleming, I., Paquette, L. A., Eds.; Pergamon Press: New York, 1991; Vol. 5, p 315.

(2) Letourneau, J. E.; Wellman, M. A.; Burnell, J. D. *J. Org. Chem.* **1997**, *62*, 7272. Wellman, M. A.; Burry, L. C.; Letourneau, J. E.; Bridson, J. N.; Miller, D. O.; Burnell, D. J. *J. Org. Chem.* **1997**, *62*, 939. Crisp, G. T.; Gebauer, M. G. *J. Org. Chem.* **1996**, *61*, 8425. Gandolfi, R.; Amade, M. S.; Rastelli, A.; Bagatti, M.; Montanari, D. *Tetrahedron Lett.* **1996**, *37*, 517.

(3) Paquette, L. A.; Gugelchuk, M. *J. Org. Chem.* **1988**, *53*, 1835. Gleiter, R.; Paquette, L. A. *Acc. Chem. Res.* **1983**, *16*, 328.

(4) Coxon, J. M.; McDonald, D. Q. *Tetrahedron Lett.* **1992**, *33*, 651.

(5) Gleiter, R.; Ginsburg, D. *Pure Appl. Chem.* **1979**, *51*, 1301.

(6) Brown, F. K.; Houk, K. N. *J. Am. Chem. Soc.* **1985**, *107*, 1971.

(7) Brown, F. K.; Houk, K. N.; Burnell, D. J.; Valenta, Z. *J. Org. Chem.* **1987**, *52*, 3050. Coxon, J. M.; Froese, R. D. J.; Ganguly, B.; Marchand, A. P.; Morokuma, K. *Synlett* **1999**, 1681.

(8) Kahn, S. D.; Hehre, W. J. *J. Am. Chem. Soc.* **1987**, *109*, 663.

(9) Williamson, K. L.; Hsu, Y.-F.; Lacko, R.; Youn, C. H. *J. Am. Chem. Soc.* **1969**, *91*, 6129. Williamson, K. L.; Hsu, Y.-F. *J. Am. Chem. Soc.* **1970**, *92*, 7385.

(10) Assteld, X.; Ruiz-Lopez, M. F.; Garcia, J. I.; Mayoral, J. A.; Salvatella, L. *Chem. Commun.* **1995**, 1371.

(11) Hagenbuch, J.-P.; Vogel, P.; Pinkerton, A. A.; Schwarzenbach, D. *Helv. Chim. Acta* **1981**, *64*, 1818.

(12) Winstein, S.; Shatavsky, M.; Norton, C.; Woodward, R. B. *J. Am. Chem. Soc.* **1955**, *77*, 4183.

(13) Macaulay, J. B.; Fallis, A. G. *J. Am. Chem. Soc.* **1988**, *110*, 4074.

(14) Fisher, M. J.; Hehre, W. J.; Kahn, S. D.; Overman, L. E. *J. Am. Chem. Soc.* **1988**, *110*, 4625.

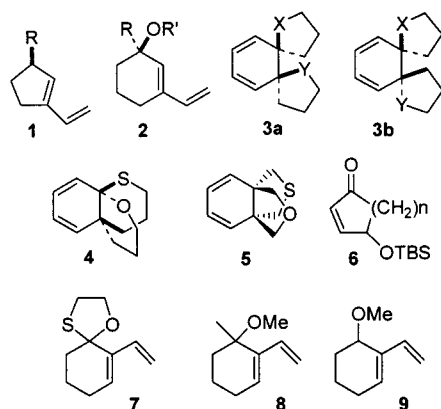


Figure 1. Structures of the dienes **1–9**.

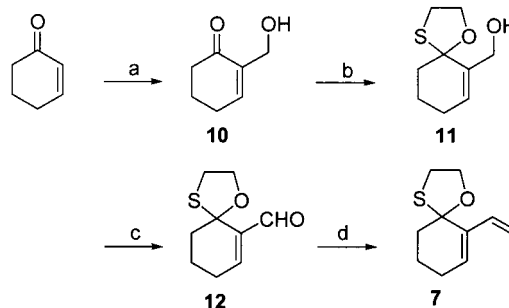
the facial selectivities of the dienes **2** and proposed the existence of a balance of electronic and steric forces that controlled the selectivity. The steric effects, however, dominated.

Paquette¹⁵ has explained the cycloaddition of several dienophiles to the dispiro-1,3-cyclohexadienes **3** from a consideration of the partial Mulliken charges on the hydrogen, carbon, and nitrogen atoms. Whereas the hydrogen and carbon atoms of the carbon–carbon double bond in NMM had positive charge, MTAD had a slightly positive charge on the doubly bonded nitrogen atoms and a negative charge in the region of the nitrogen lone pairs. Also, the partial charges on the atoms of interest in the diene were calculated to be (O) -0.25 , (S) $+0.14$, and (CH_2 , bonded to the cyclohexadiene ring carbon bearing the heteroatom), $+0.10$. It is evident from these charges that the oxygen in **3** will have a stabilizing effect with NPM in the *syn* approach. Hence, the *syn* cycloadducts were the major or single product. A similar argument favors *anti* addition of MTAD as was indeed observed. Two important points had emerged: (a) proximity to oxygen results in the onset of electrostatic factors, and (b) in a competition between S and CH_2 , the larger steric factor of S dominates.

The above electrostatic model, however, failed to explain the preferred *syn*-to-O addition of MTAD to **3b** ($\text{X} = \text{O}$, $\text{Y} = \text{S}$); the model predicted addition *syn* to S. This anomaly was attributed to the large steric bulk of S that guided the reaction *anti* to it. This had also explained the exclusively *syn*-to-O addition of MTAD to the tricyclic diene **4**.¹⁶ In contrast, the propelladiene **5** underwent cycloaddition exclusively *syn* to S, which was attributed to secondary orbital effects by Ginsburg.¹⁷

In brief, the origin of π -selectivity has been rationalized sometimes as a consequence of purely electronic effects,^{11,12} sometimes purely steric effects,^{13,14} and sometimes a combination of both.^{15,16} Rokach has even concluded that there is no such effect of heteroatom substituent(s) on the dienophile and that only such substituents on the diene contribute to the facial selectivity.¹⁸ These results contradict the findings of Danishefsky,¹⁹ who achieved very good *syn* selection from the

Scheme 1. Synthesis of **7**^a



^a Reagents: (a) aqueous HCHO , DMAP, THF; (b) $\text{HSCH}_2\text{CH}_2\text{OH}$, PPTS, C_6H_6 , reflux; (c) PDC, CH_2Cl_2 ; (d) $\text{Ph}_3\text{P}^+\text{CH}_3\text{I}^-$, *n*-BuLi, THF, 0°C .

AlCl_3 -catalyzed DA cycloadditions of 1,3-butadiene to **6** ($n = 1, 2$). It is clear from these contradicting reports that the facial control elements are not yet properly understood and, therefore, more studies are desirable.

In continuation of our studies on the facial effect of the 1-oxa-4-thiolan function,²⁰ we have studied the selectivities of 1-oxa-4-thia-6-vinylspiro[4.5]dec-6-ene (**7**), 3-methoxy-3-methyl-2-vinylcyclohexene (**8**), and 3-methoxy-2-vinylcyclohexene (**9**). The σ bonds formed from a DA cycloaddition are 1,3/1,4 from the stereogenic center. In the examples studied earlier by others, the bonds formed are either 1,2/1,2 or 1,2/1,5 from the stereogenic center.

Starting Materials and Diastereomer Analysis

The diene **7** was synthesized as shown in Scheme 1. Baylis–Hillman reaction of 2-cyclohexenone with formalin using a literature protocol²¹ furnished **10**. The condensation of **10** with 2-mercaptoethanol was effected in benzene at reflux under a Dean–Stark setup to obtain the monothioacetal **11**. This, on oxidation with PDC in CH_2Cl_2 ,²² furnished the aldehyde **12**. Wittig olefination with the lithium salt of methyltriphenylphosphonium iodide in THF at 0°C gave the diene **7** that was stored at -10°C for a week with very little decomposition.

The dienes **8** and **9** were synthesized from **17**, which, in turn, was prepared as shown in Scheme 2. The ketone **17** was reacted with MeMgI in Et_2O , and the resultant alcohol was O-methylated to **8**. Further, the reduction of **17** with LiAlH_4 in Et_2O and O-methylation of the resultant alcohol furnished **9**.

All the dienophiles used in the present study were used as received from Aldrich Chemical Co. The distribution of the diastereomers formed from DA cycloadditions was calculated from the integrals of the vinylic hydrogen atoms and also OMe. The relative stereochemical characterizations were made from the chemical shifts of the vinylic hydrogen atoms and the X-ray structural data of several DA cycloadducts and their derivatives.

(14) Datta, S. C.; Franck, R. W.; Tripathy, R.; Quigley, G. J.; Huang, L.; Chen, S.; Sihaed, A. *J. Am. Chem. Soc.* **1990**, *112*, 8472.

(15) Paquette, L. A.; Branan, B. M.; Rogers, R. D.; Bond, A. H.; Lange, H.; Gleiter, R. *J. Am. Chem. Soc.* **1995**, *117*, 5992.

(16) Branan, B. M.; Paquette, L. A. *J. Am. Chem. Soc.* **1994**, *116*, 7658.

(17) Ginsburg, D. *Tetrahedron* **1983**, *39*, 2025.

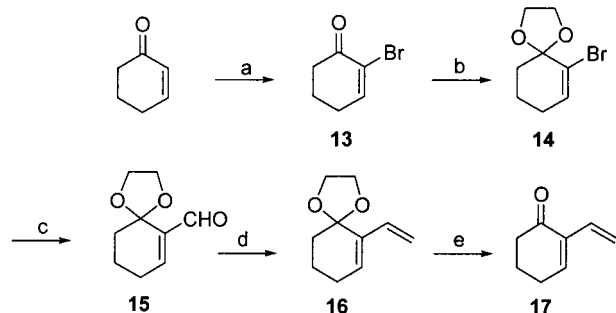
(18) Pudukulathan, Z.; Manna, S.; Hwang, S. W.; Khanapure, S. P.; Lawson, J. A.; FitzGerald, G. A.; Rokach, J. *J. Am. Chem. Soc.* **1998**, *120*, 11953.

(19) Danishefsky, S. J.; Paz Cabal, M.; Chow, K. *J. Am. Chem. Soc.* **1989**, *111*, 3456.

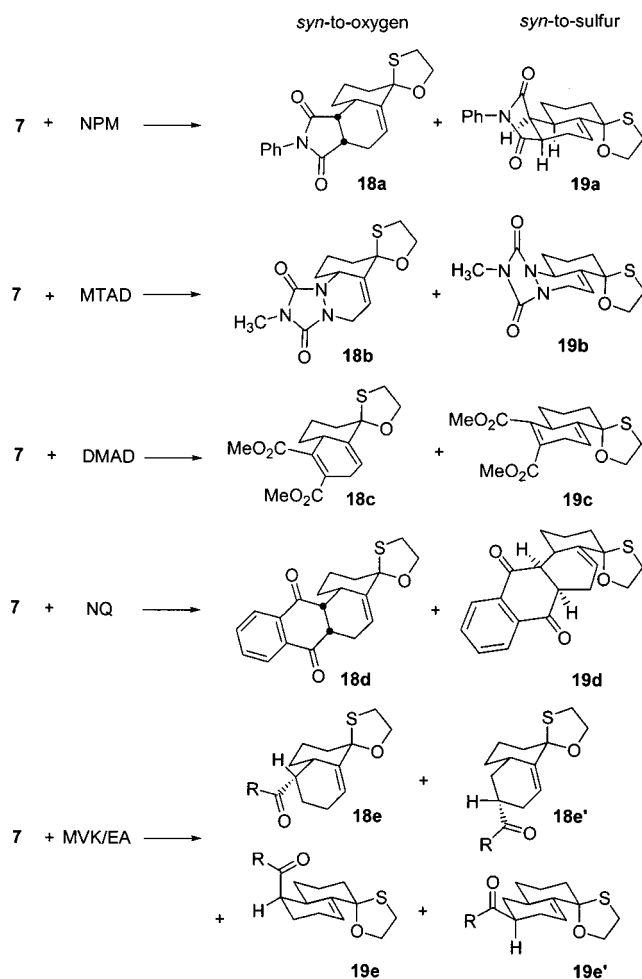
(20) Jeyaraj, D. A.; Yadav, V. K.; Parvez, M.; Gauniyal, H. M. *J. Org. Chem.* **1998**, *63*, 3831. Yadav, V. K.; Jeyaraj, D. A.; Parvez, M.; Yamdagni, R. *J. Org. Chem.* **1999**, *64*, 2928. Yadav, V. K.; Jeyaraj, D. A.; Parvez, M. *J. Chem. Soc., Perkin Trans. 1* **2000**, 1423.

(21) Rezgui, F.; El Gaied, M. M. *Tetrahedron Lett.* **1998**, *39*, 5965.

(22) Furniss, B. S.; Hannaford, A. J.; Smith, P. W. G.; Tatchell, A. R. *Vogel's Textbook of Practical Organic Chemistry*; Longman Group: Harlow, U.K., 1989.

Scheme 2. Synthesis of the Ketone **17**, the Precursor of the Dienes **8** and **9**^a

^a Reagents: (a) Br₂, Et₃N, CCl₄, 0 °C to rt; (b) HOCH₂CH₂OH, *p*-TSA, C₆H₆, reflux; (c) *n*-BuLi, HCONMe₂, –80 °C; (d) CH₂=PPh₃, 0 °C to rt; (e) *p*-TSA, acetone, rt.

Scheme 3. Diels–Alder Cycloadducts of **7** with Selected Dienophiles

Results and Discussion

The DA cycloadditions of various dienophiles to **7** were carried out both thermally and in the presence of selected Lewis acids. The reactions and their products are collected in Scheme 3 and the stereochemical results in Table 1. We present below a detailed account of these reactions.

Diels–Alder Additions under Thermal Conditions. The diene **7** reacted with NPM in toluene at 40 °C to furnish a mixture of two adducts in an 8:1 ratio (entry 1).²³ The vinylic H of the minor adduct appeared

Table 1. Stereochemical Results and the Product Distribution from the Diels–Alder Additions of **7** to Selected Dienophiles under Thermal and Lewis Acid Conditions

entry	dienophile	reaction conditions	time	yield (%)	ratio 18:19
1	NPM	40 °C, toluene	11 h	99	8.0:1.0
2	NPM	rt, 4 M LPNM	6 h	99	2.2:1.0
3	MTAD	70 °C to rt, DCM:THF = 1:1	4 h	99	10.0:1.0
4	MTAD	rt, 4 M LPNM		decomposition of MTAD	
5	DMAD	40 °C, toluene	42 h	93	1.0:1.7
6	DMAD	reflux, toluene	6 h	76	1.0:1.4
7	DMAD	rt, 4 M LPNM	3 h	99	2.5:1.0
8	DMAD	rt, nitromethane	6 h	99	0.5:1.0
9	DMAD	rt, 4 M LPDE	12 h		1.5:1.0
10	NQ	rt, toluene	24 h	no reaction	
11	NQ	rt, 4 M LPNM	5 h	50	3.6:1.0
12	MVK	rt, toluene	7 d	99	1.0:1.0
13	MVK	110 °C, toluene	12 h	60	2.0:1.0
14	MVK	rt, 4 M LPNM	4 h	99	6.0:1.0
15	MVK	0 °C, 4 M LPNM	6 h	99	7.2:1.0
16	MVK	rt, 1 M LiClO ₄ /CH ₃ CN	12 h	99	3.6:1.0
17	MVK	rt, 1 M LiBF ₄ /CH ₃ CN	4 h	95	5.6:1.0
18	MVK	rt, 4 M LPDE	6 h	90	8.8:1.0
19	EA	rt, toluene	24 h	no reaction	
20	EA	110 °C, toluene	24 h	63	1.6:1.0
21	EA	rt, 4 M LPNM	12 h	99	1.0:0.0
22	EA	rt, 4 M LPDE	16	92	9.5:1.0

at δ 6.16 (t, J = 4.2 Hz) and that of the major adduct at δ 5.82 (t, J = 3.9 Hz). These adducts were separated by radial chromatography. The stereochemical assignment of the major adduct was secured as in **18a**, a product of *endo*-addition *syn* to O, from its X-ray crystal data. Likewise, the stereostructure of the minor adduct was confirmed as in **19a**, a product of *endo*-addition *syn* to S, from its X-ray crystal data.

The cycloaddition of MTAD at –70 °C in a 1:1 mixture of THF and CH₂Cl₂ gave a mixture of two adducts in a 10:1 ratio (entry 3). The vinylic hydrogens appeared at δ 6.39 (t, J = 2.4 Hz, minor) and δ 5.81 (t, J = 1.8 Hz, major). Our all attempts to separate the two adducts by chromatography failed. However, a recrystallization from MeOH–CH₂Cl₂ furnished crystals of the major adduct that had, from its X-ray crystal data, the stereostructure shown in **18b**. The cycloaddition, therefore, had proceeded predominantly *syn* to O via an *endo*-TS. The minor adduct must, therefore, be the product of *endo*-addition *syn* to S and possess the stereostructure **19b** in accordance with the results obtained from the cycloaddition of NPM above.

DMAD reacted with the diene at 40 °C in toluene to provide a mixture of two separable adducts in a 1:1.7 ratio (entry 5). The vinylic H appeared at δ 5.66 (t, J = 3.4 Hz) in the minor adduct and at δ 6.25 (t, J = 3.0 Hz) in the major adduct. The major adduct that was recrystallized from EtOAc–hexanes had the stereostructure **19c** from its X-ray structural data. The major adduct, therefore, is derived from addition *syn* to S. It is significant to note the S in **19c** is disposed equatorially. The minor adduct, therefore, must have the stereostructure **18c**. When compared to the reactions with NPM and MTAD above, the reversal in selectivity in the cycloaddition of DMAD is obvious. The *syn*-to-O cycloaddition was somewhat enhanced to **18c**:**19c** = 1:1.4 on carrying out the reaction in toluene at reflux (entry 6).

(23) We observe only kinetic products. This conclusion was made from separate experiments that involved heating a solution of each adduct of NPM with **7** in toluene for 5 h. There was no change in either instance.

The cycloaddition of NQ in toluene at 25 °C failed, and neither **18d** nor **19d** was formed (entry 10). At higher temperatures there was extensive decomposition.

The DA cycloadditions of unsymmetrical dienophiles were also attempted. MVK reacted very slowly (toluene, 7 days, 25 °C) and furnished a mixture of four adducts. Clearly, the cycloaddition had proceeded *syn* to both oxygen and sulfur through regioisomeric TSs. The chemical shift of the vinylic H of each adduct was different from those of the others, and these appeared in two sets. Two adducts had the vinylic H atoms at δ 6.36 and 6.26, a region where the *syn*-to-S adducts **19e** and **19e'** will be expected. The other set had the vinylic H atoms at δ 5.74 and 5.69, a region where the *syn*-to-O adducts **18e** and **18e'** will be expected. The ratio of the two sets of adducts was 1:1 (entry 12), and their separation was difficult. A moderate enhancement in *syn*-to-O selectivity to 2:1 was, however, observed when the cycloaddition was carried out in a sealed tube at 110 °C (entry 13).

EA did not add to **7** at 25 °C (entry 19). However, four adducts had formed when the reaction mixture was heated to 110 °C in a sealed tube. The trend for the chemical shifts of the vinylic H atoms was similar to those of the MVK cycloadducts. A similar calculation of the ratio (1.6:1, entry 20) showed a marginal selectivity in favor of *syn*-to-O addition.

Diels–Alder Cycloadditions under Catalysis by LPNM. We turned our attention next to Lewis acid-catalyzed DA cycloadditions that are reported to proceed at low temperatures with high regio-, stereo-, and enantiocontrol.²⁴ Recently, the use of LiClO₄ in carbon–carbon bond formation reactions has gained much significance. A solution of LiClO₄ in Et₂O or CH₃NO₂ is very effective in catalyzing Claisen,²⁵ Michael,²⁶ and DA cycloadditions.^{27a} The rationale for the catalytic activity of LiClO₄ has been disputed. Grieco et al.^{27a,b} have suggested the large internal pressure caused by the change in solvent structure that induces a compression of the reactants as the rationale for the observed rate acceleration. Braun and Sauer²⁸ have attributed the rate acceleration to polar solvent effects. Forman and Dailey²⁹ have presented evidence in favor of the catalytic effect of Li⁺. It is now generally accepted that both the medium effect and Li⁺ are responsible for the said catalytic activity.

We chose to explore DA cycloadditions to **7** in 4 M LPNM mostly as it is essentially a neutral medium.²⁶ An increase in the rate of cycloaddition of DMAD to **7** at 25 °C was evident from its completion in <3 h (entry 7). ¹H NMR analysis of the product mixture showed it to favor *syn*-to-O addition (**18c**:**19c** = 2.5:1). This selectivity is opposite that of the normal reaction that favored addition *syn* to S (entries 5–8). To assess the contribution of the solvent to the facial control, the reaction was carried out in CH₃NO₂ at 25 °C without any LiClO₄. The reaction furnished a diastereomeric ratio of 0.5:1 (entry 8) that compared favorably with the 0.6:1 selectivity observed from the reaction in toluene at 40 °C (entry 5). Thus, the *syn*-to-O addition in LPNM was due primarily to LiClO₄.

NQ reacted smoothly in LPNM to furnish a mixture of two adducts in a 3.6:1 ratio (entry 11). ¹H chemical shift data of the vinylic H atoms (major adduct, δ 5.75; minor adduct, δ 6.34) indicated the dominance of *syn*-to-O addition. It is significant to recall that NQ had not reacted with **7** in toluene at 25 °C. Our attempts to separate the isomers by chromatography over silica gel resulted in extensive decomposition. Fractional recrystallization also failed to furnish a pure sample of either adduct.

The reaction with MVK proceeded readily with high stereocontrol, regiocontrol, and facial control. From the three adducts that were formed, one was present in large excess of the other two. The ratio 6:1 calculated as before from the ¹H chemical shifts favored addition *syn* to O (entry 14). A recrystallization from EtOAc–hexanes furnished the most major adduct, which, from its X-ray structural data, was **18e** (R = Me). This isomer had the vinylic H at δ 5.69. The other *syn*-to-O adduct displayed the vinylic H at δ 5.74, probably having the structure **18e'** (R = Me). Both **18e** and **18e'** are the products of the corresponding *endo*-TSs.

The cycloaddition of EA was even more selective than the addition of MVK as it gave only one of the total four adducts possible (entry 21). This adduct displayed the vinylic H at δ 5.66 that corresponded very well with that of **18e** (R = Me, δ 5.69). This product must, therefore, be **18e** (R = OEt). This material and the corresponding alcohol were liquids. We did not succeed in making a suitable crystalline derivative of the alcohol either.

We have compared the catalytic activity of LPNM to those of LPDE and LiBF₄.³⁰ The *syn*-to-O addition was favored in all the cases. The selectivity of MVK addition in LPDE (8.8:1.0, entry 18) was better than that in LPNM (6:1, entry 14). DMAD and EA, however, showed somewhat poor selectivity in LPDE compared to LPNM (cf. entries 7 and 21 with entries 9 and 22, respectively). The selectivity of MVK addition catalyzed by 1 M LiBF₄ in CH₃CN (5.6:1.0, entry 17) was comparable to that of the 4 M LPNM-catalyzed addition (6.0:1.0, entry 14).

Ab Initio MO Investigations. We have computed the ground-state geometry of **7** using DFT *ab initio* MO methods at the Becke3LYP/6-31+G* level.³¹ It could be an equilibrium mixture of the two conformers **7a** and **7b** (Figure 2). Conformer **7a** is 0.18 kcal mol⁻¹ more stable than conformer **7b**. This energy difference translates into a 1.4:1 distribution of **7a** and **7b** at 25 °C, respectively. The diene moiety is not planar in either conformer. The plane of the external olefin is 32.6° toward S from the plane of the ring olefin in **7a** and 42° toward oxygen in **7b**.

The *syn*-to-O addition to **7a** requires an axial carbon–carbon bond formation on C7. However, the *syn*-to-S addition to **7a** requires the formation of an equatorial carbon–carbon bond. Since the formation of an axial bond

(24) Yates, P.; Eaton, P. E. *J. Am. Chem. Soc.* **1960**, *82*, 4436.

(25) Grieco, P. A.; Clark, J. D.; Jagoe, C. T. *J. Am. Chem. Soc.* **1991**, *113*, 5488.

(26) Saraswathy, V. G.; Sankararaman, S. *J. Org. Chem.* **1995**, *60*, 5024.

(27) (a) Grieco, P. A.; Nunes, J. J.; Gaul, M. D. *J. Am. Chem. Soc.* **1990**, *112*, 4595. (b) Kumar, A. *J. Org. Chem.* **1994**, *59*, 4612.

(28) Braun, S.; Sauer, J. *Chem. Ber.* **1986**, *119*, 1269.

(29) Forman, M. A.; Dailey, W. P. *J. Am. Chem. Soc.* **1991**, *113*, 2761.

(30) Smith, D. A.; Houk, K. N. *Tetrahedron Lett.* **1991**, *32*, 1549. Babu, B. S.; Balasubramanian, K. K. *Synlett* **1999**, 1261.

(31) All the geometry optimizations and the calculations of anti-periplanar effects were performed at the Becke3LYP/6-31G* level using the program GAUSSIAN 94, Revision C.2: Frisch, M. J.; Trucks, G. W.; Schlegel, H. B.; Jones, P. M. W.; Johnson, B. G.; Robb, M. A.; Cheeseman, J. R.; Keith, T.; Petersson, G. A.; Montgomery, J. A.; Raghavachari, K.; Al-Laham, M. A.; Zakrzewski, V. G.; Ortiz, J. V.; Foresman, J. B.; Cioslowski, J.; Stefanov, B. B.; Nanayakkara, A.; Challacombe, M.; Peng, C. Y.; Ayala, P. Y.; Chen, W.; Wong, M. W.; Andres, J. L.; Replogle, E. S.; Gomperts, R.; Martin, R. L.; Fox, D. J.; Binkley, J. S.; Defrees, D. J.; Baker, J.; Stewart, J. P.; Head-Gordon, M.; Gonzalez, C.; Pople, J. A., Gaussian, Inc., Pittsburgh, PA, 1995.

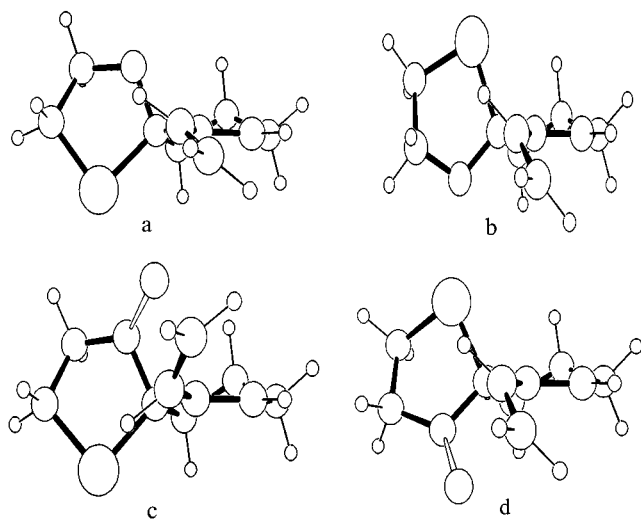


Figure 2. Ab initio MO conformers of **7**: (a) **7a**; (b) **7b**; (c) **7a**–Li⁺; (d) **7b**–Li⁺.

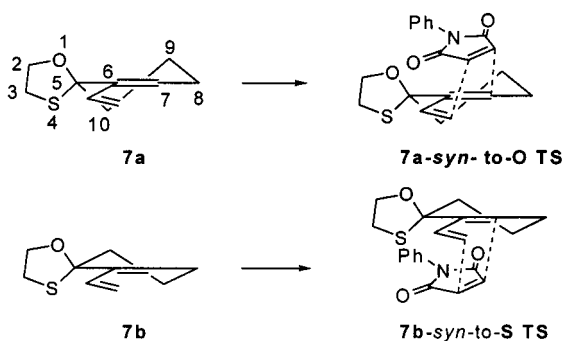


Figure 3. Preferred transition states for DA addition to **7a** and **7b**.

is favored over an equatorial bond from stereoelectronic considerations,³² **7a** undergoes addition *syn* to O. Similarly, **7b** undergoes addition *syn* to S. If we presume that the activation energies for the reactions of both **7a** and **7b** are equal, the ratio of the two adducts must reflect the above **7a**:**7b** ratio. This, however, is not so. The *syn*-to-O addition takes place in far excess of the calculated value.

The TSs for additions to **7a** and **7b** are given in Figure 3. These transition states (and the resultant adducts), however, suffer from 1,3-diaxial interactions of the axial acetal heteroatom with the axial carbon–carbon bond formed on C7. The larger steric interactions with S in the TS for addition to **7b** is likely to favor addition to **7a** wherein such steric interactions are relatively less. Further, these 1,3-diaxial interactions may also induce a ring flip in the product. As a consequence, a *syn*-to-O adduct from **7a** will have the C–O and C–S bonds, respectively, equatorial and axial. The reverse applies to a *syn*-to-S adduct formed from **7b**. This is indeed observed from the X-ray structures of **18a**, **19a**, **18b**, **18e**, and **19c** (see the Supporting Information). It is interesting to note that one may arrive at these conclusions by invoking the formation of an equatorial carbon–carbon bond on C7

as well. This, however, does not conform to the stereoelectronic effects.

The preferential *syn*-to-S addition of DMAD appears to be a consequence of electrostatic repulsion of an electron pair of acetal oxygen with the orthogonal π -orbital of the acetylene unit. The magnitude of this interaction, however, is expected to be low because the interacting orbitals are somewhat away from each other in the TS for addition. As a result, the preference for *syn*-to-S addition is likely not very high. Similar interactions involving an electron pair of sulfur in **7b** and the acetylene unit will not be possible because of an energy mismatch. The energy of the π -orbital of acetylene is closer to that of the 2p electron pairs of oxygen than those of S.³³ An explanation based on such n – π interactions has been invoked previously.^{21,34}

The cycloaddition of DMAD is predominantly *syn* to O in LPNM. This suggests a possible coordination of Li⁺ to an electron pair of the acetal oxygen that eliminates the above electrostatic repulsion and, thus, allows the addition to proceed *syn* to O. An extended coordination of Li⁺ with an ester function of DMAD will accelerate the addition. In practice, the *syn*-to-O addition was favored only by a factor of 2.5 over the *syn*-to-S addition. The low selectivity is likely due to the increased steric encumbrance caused by Li⁺–oxygen combination on the face *syn* to O. Such a rationale receives good support from the observation that the *syn*-to-O addition of NPM was reduced from 8.0:1.0 in toluene to 2.2:1.0 in LPNM. The large size of the phenyl ring comes close to the Li⁺–oxygen combination in the *syn*-to-O addition and results in unfavorable steric interactions. Such steric interactions will, however, be less important for small dienophiles such as EA and MVK, and thus, predominantly *syn*-to-O addition will be expected. This is observed indeed from the present experiments (vide supra).

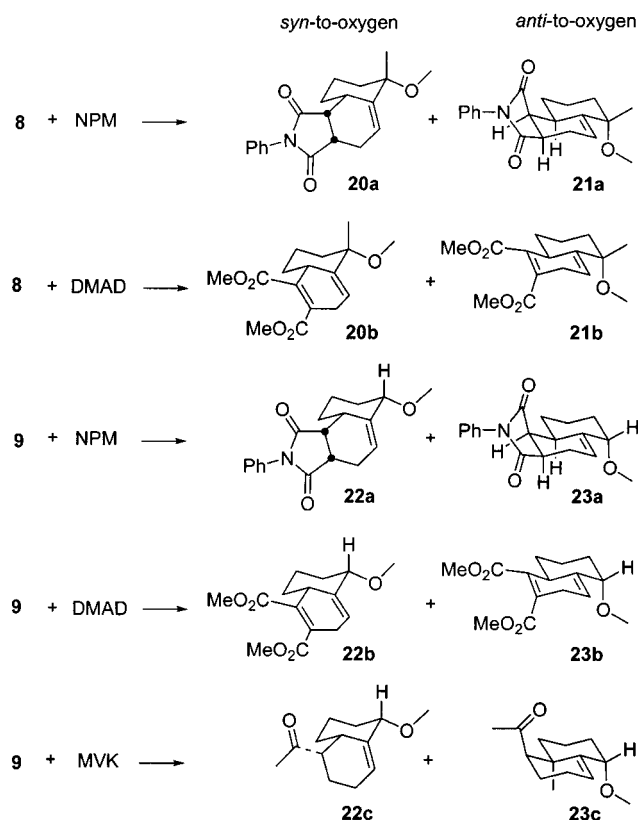
We have computed the effect of coordination of Li⁺ with the acetal oxygen on the geometry of **7**. The oxygen electron pair that was closer to the diene function was allowed for the said coordination. The geometrical changes are very significant and interesting. In **7a**–Li⁺ (Figure 2c), the external olefin has moved 40.3° upward and close to O/Li⁺. Likewise, the external olefin has moved 46.1° downward, close to O/Li⁺, in **7b**–Li⁺ (Figure 2d). Conformer **7a**–Li⁺ is 0.05 kcal mol^{–1} more stable than conformer **7b**–Li⁺. This small energy difference allows for an almost equal equilibrium concentration of the two species. The extended coordination of Li⁺ with a dienophile will allow the addition *syn* to O in both the species. For the fact that an axial carbon–carbon bond formation on C7 is favored over that of an equatorial bond, we believe that most of the *syn*-to-O product is formed from **7a**–Li⁺. Though the addition *syn* to S in **7b**–Li⁺ involves an axial carbon–carbon bond formation on C7, it suffers from (a) 1,3-diaxial interactions arising from the sulfur and (b) the absence of proximity of the two addends arising from the coordination of Li⁺ with both the diene and the dienophile.

More Diels–Alder Additions. We have studied DA cycloadditions to the dienes **8** and **9** as well (Scheme 4).

(33) Coxon, J. M.; MacLagan, R. G. A. R.; McDonald, D. Q.; Steel, P. J. *J. Org. Chem.* **1991**, *56*, 2542.

(34) Fessner, W. D.; Scheumann, K.; Prinzbach, H. *Tetrahedron Lett.* **1991**, *32*, 5939. Coxon, J. M.; O'Connell, M. J.; Steel, P. J. *J. Org. Chem.* **1987**, *52*, 4726. Coxon, J. M.; Fong, S. T.; McDonald, D. Q.; Steel, P. J. *Tetrahedron Lett.* **1993**, *34*, 163. Mehta, G.; Uma, R. *Tetrahedron Lett.* **1995**, *36*, 4873. Mehta, G.; Uma, R. *J. Org. Chem.* **2000**, *65*, 1685.

(32) Deslongchamps, P. In *Stereoelectronic Effects in Organic Chemistry*; Baldwin, J. E., Ed.; Pergamon: New York, 1983; Vol. 1, Chapters 2 and 3. Newitt, L. A.; Steel, P. G. *J. Chem. Soc., Perkin Trans. 1* **1997**, 2033. Adcock, W.; Cotton, J.; N. R.; Trout, N. A. *J. Org. Chem.* **1994**, *59*, 1867.

Scheme 4. Diels–Alder Cycloadducts of 8 and 9 with Selected Dienophiles


These dienes differ from Franck's diene **2** with respect to the location of the external olefinic bond. The steric factor being the lone factor for facial discrimination, one would expect the *anti*-to-OMe addition to prevail but only to the extent that the difference of the substituents' n values³⁵ would permit. With a dienophile such as DMAD that is less susceptible to steric interactions, repulsive interactions are likely to control the addition and allow it to proceed preferably *anti* to OMe. Both **8** and **9** may, therefore, exhibit very similar selectivities in their DA cycloadditions to DMAD. Further, the *anti*-to-OMe addition of a sterically susceptible dienophile such as NPM must increase from **8** to **9**.

The substrates **8** and **9**, however, could exist as an equilibrium mixture of the equivalents of **7a** and **7b**. Conformers **8a** and **9a** are 2.98 and 0.98 kcal mol⁻¹ more stable than conformers **8b** and **9b**, respectively (Figure 4). Thus, **8a/9a** prevailing over **8b/9b**, the preference for DA cycloadditions *anti* to OMe must indeed be a consequence of steric effects. The experimental selectivities of the substrates **8** and **9** are collected in Table 2.

Both **8** and **9** showed similar *anti*-to-OMe addition of DMAD. The *anti*-to-OMe addition of NPM is larger with **9** than with **8**. This is in accordance with the above analysis, and it follows the steric control model of facial selection. The cycloadditions of DMAD and MVK to **9** in LPNM at room temperature proceeded largely *syn* to O to furnish 2.1:1 and >10:1 product distributions. In contrast, MVK did not react with **9** in toluene at room temperature, and it furnished a mixture of several adducts when refluxed in a sealed tube. The enhanced

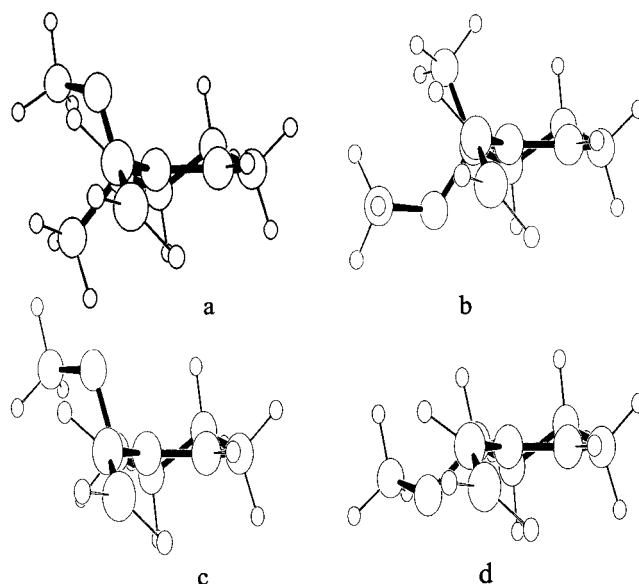


Figure 4. Ab initio MO conformers: (a) **8a**; (b) **8b**; (c) **9a**; (d) **9b**.

Table 2. Stereochemical Results and Product Distribution from the Diels–Alder Additions of the Dienes 8 and 9 to Selected Dienophiles under Thermal and Lewis Acid Conditions

entry	reaction	reaction conditions	time	yield (%)	ratio <i>syn:anti</i> O
1	8 + NPM	40 °C, toluene	33 h	90+	1.0:1.1
2	8 + DMAD	reflux, toluene	6 h	90+	1.0:1.6
3	9 + NPM	40 °C, toluene	24 h	90+	1.0:4.3
4	9 + DMAD	reflux, toluene	6 h	90+	1.0:1.8
5	9 + DMAD	rt, 4 M LPNM	6 h	90+	2.1:1.0
6	9 + MVK	rt, 4 M LPNM	4 h	90+	>10:1.0

Table 3. Stereochemical Characterization of the Products from the ¹H Chemical Shifts (δ) of the Vinylic Hydrogens and OMe

reaction	δ _{vinylic} H		δ _{OMe}	
	<i>syn</i> to O	<i>anti</i> to O	<i>syn</i> to O	<i>anti</i> to O
7 + NPM	5.82	6.16		
7 + MTAD	5.81	6.39		
7 + DMAD	5.66	6.25		
7 + NQ	5.75	6.34		
7 + MVK	5.69/5.74	6.26/6.36		
7 + EA	5.66/5.74	6.25/6.37		
8 + NPM	5.93	5.66	3.07	3.02
8 + DMAD	5.73	5.59	3.32	3.06
9 + NPM	5.72	5.70	3.31	3.21
9 + DMAD	5.64	5.59	3.42	3.19
9 + MVK	5.62	5.62	3.42	3.23

syn-to-O addition to **9** in LPNM can be easily explained by invoking coordination of Li⁺ to the oxygen and its extended coordination with DMAD and MVK. It is important to note that this extended coordination will also improve the regioselectivities of monofunctional dienophiles. The crystal structure of the *anti*-to-O adduct of NPM with **9** shows that it is a product of *endo*-addition wherein the OMe is disposed axially.

¹H Chemical Shifts of the Vinylic Hydrogen and OMe as Probes to Stereochemical Characterization.

The chemical shifts of the vinylic H and OMe in the DA cycloadducts prepared in the present study are collected in Table 3. The vinylic H in the *syn*-to-O adduct of **7** appeared at a lower δ value than the vinylic H in the *syn*-to-S adduct. While the vinylic H is close to the

(35) Forster, H.; Vogtle, F. *Angew. Chem., Int. Ed. Engl.* **1977**, *16*, 429.

acetal oxygen in the former, it is close to the acetal S in the latter. The larger δ value of the vinylic H in the *syn*-to-O adducts of **8** and **9** is likely due to its proximity to OMe. Further, the OMe in the *syn*-to-O adduct is somewhat deshielded compared to the OMe in the *anti*-to-O adduct. This is likely due to the anisotropic effect of the olefin to which the OMe has better proximity in the *syn*-to-O adduct than the OMe in the corresponding *anti* adduct.

Conclusions

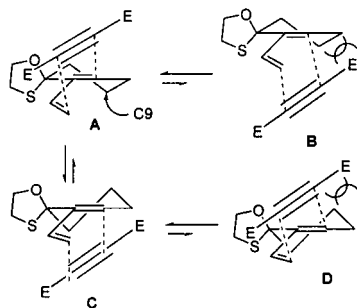
The preferred *syn*-to-O selectivity in the DA cycloadditions to **7** is due largely to the steric encumbrance caused by the large sulfur atom. The reversal in selectivity in the addition of DMAD to **7** has its origin in the electrostatic repulsion between an electron pair orbital of the acetal oxygen and the orthogonal π -orbital of the acetylene unit in DMAD.³⁶ LPNM helps the additions of sterically less sensitive dienophiles to **7** to proceed *syn* to O by promoting coordination of Li⁺ to the acetal oxygen and the dienophile. Additionally, the coordination of Li⁺ with the dienophile improves the regioselectivity of addition of monofunctional dienophiles as well. The dienes **8** and **9** exhibited a preference for *anti*-to-O addition that is a consequence of the relative steric effects of the substituents. This selectivity, however, reversed as expected when the addition was carried out in LPNM.

The Cieplak model³⁷ favors bond construction *anti* to the more electron-donating of the C–O and C–S bonds. Since a C–S bond is more electron-donating than a C–O bond, a dominant *anti*-to-S selectivity of **7** with dienophiles such as NPM, MTAD, and EA would appear to follow. However, the preferred *syn*-to-S addition of DMAD (Table 1, entry 5) and lack of facial discrimination by MVK at room temperature (Table 1, entry 12) are not explained. The preferred *anti*-to-OMe additions to **8** and **9** also do not obey the Cieplak model. Both a C–C bond and a C–H bond on the stereogenic centers in **8** and **9**, respectively, are more electron-donating than the C–O bond on the same center.

Experimental Section

¹H and ¹³C NMR spectra were recorded using solutions in CDCl₃. The ¹H and ¹³C spectra are referred, respectively, to

(36) In the view of one reviewer, an alternate explanation to the reversal in selectivity of DMAD addition to **7** is as follows. Sulfur no longer imposes a significant steric difference between the two faces. Instead, the energy difference between **A** and **C** given below is likely to be in the same order as the difference between **7a** and **7b** because the steric bias of sulfur is rendered negligible by the linearity of DMAD. The small difference in selectivity in this case is due to a preference for addition to the face away from the C9 methylene (**A** vs **B** and **C** vs **D**) residue and the small difference in energy between **A** and **C**. The ratios of products (1:1.7 at 40 °C and 1:1.4 at 110 °C) are close to the calculated ratio for **7a** and **7b** (1:1.4 for a 0.18 kcal mol^{−1} difference).



(37) Cieplak, A. S. *J. Am. Chem. Soc.* **1981**, *103*, 4540. Cieplak, A. S.; Tait, B. D.; Johnson, C. R. *J. Am. Chem. Soc.* **1989**, *111*, 8447.

TMS used as an internal standard and the central line for CDCl₃. IR spectra were recorded on a Perkin-Elmer 1320 infrared spectrophotometer. Melting points are uncorrected. Column chromatography was performed over silica gel (100–200 mesh) using petroleum ether (bp 60–80 °C) and EtOAc mixtures as the eluent. The separation of the isomers and their further rigorous purification were achieved by radial chromatography using 1–2 mm thick plates coated with silica gel PF₂₅₄ (E. Merck). Solvents were removed under reduced pressure on a rotovap. The visualization of the spots on TLC was effected by UV illumination, exposure to iodine vapor, DNP solution in ethanol containing 10% H₂SO₄, and heating of the plates dipped in 10% aqueous H₂SO₄ in EtOH.

6-Hydroxymethyl-1-oxa-4-thiaspiro[4.5]dec-6-ene (**11**).

A solution of the keto alcohol **10** (630 mg, 5 mmol), 2-mercaptoethanol (365 mg, 5 mmol), and PPTS (25 mg, 0.1 mmol) in benzene (100 mL) was refluxed under N₂ under azeotropic removal of water using a Dean–Stark setup. After 10 h, the reaction mixture was cooled to rt and the solvent removed. The residue was purified by chromatography to furnish **11** (250 mg) and **10** (460 mg). ¹H NMR (400 MHz): δ 1.62–1.77 (m, 1H), 1.83–1.89 (m, 1H), 1.97–2.04 (td, J = 12, 3 Hz, 1H), 2.05–2.16 (m, 4H), 2.40–2.80 (br s, 1H), 3.08–3.13 (m, 1H), 3.17–3.24 (m, 1H), 4.04 (d, J = 12 Hz, 1H), 4.04–4.11 (dt, J = 9.5, 5.6 Hz, 1H), 4.33 (d, J = 12.2 Hz, 1H), 4.40–4.45 (m, 1H), 5.92 (t, J = 3.7 Hz, 1H). ¹³C NMR (100 MHz): δ 20.6, 24.7, 34.5, 38.4, 64.1, 70.5, 95.2, 130.7, 138.1. IR (film): 3380, 2900, 1250, 1140, 1080, 890 cm^{−1}. Anal. Calcd for C₉H₁₄O₂S: C, 58.04; H, 7.58. Found: C, 57.90; H, 7.48.

1-Oxa-4-thiaspiro[4.5]dec-6-ene-6-carbaldehyde (**12**).

To a stirred solution of pyridine (948 mg, 12 mmol) in dry CH₂Cl₂ (15 mL) was added chromium trioxide (600 mg, 6 mmol) in one portion, and the stirring was continued for 15 min. To the dark red solution was added the alcohol **11** (1 mmol, 186 mg) in CH₂Cl₂ (2 mL). An immediate black precipitation was observed. The stirring was continued for 15 min. The solvent was removed, and the residue was extracted into Et₂O. This was filtered through a short column of silica gel, and the solvent was removed. The crude residue was purified by chromatography to furnish **12** (127 mg, 71%). ¹H NMR (400 MHz): δ 1.70–1.76 (m, 1H), 1.83–1.88 (m, 1H), 2.00–2.13 (m, 2H), 2.27–2.32 (m, 2H), 3.12–3.16 (m, 1H), 3.34–3.38 (m, 1H), 4.07–4.12 (m, 1H), 4.48–4.52 (m, 1H), 6.90 (t, J = 4.0 Hz, 1H), 9.52 (s, 1H). ¹³C NMR (100 MHz): δ 20.4, 25.8, 35.1, 38.9, 71.6, 90.4, 140.3, 146.9, 191.5. Anal. Calcd for C₉H₁₂O₂S: C, 58.67; H, 6.57. Found: C, 58.52; H, 6.48.

1-Oxa-4-thia-6-vinylspiro[4.5]dec-6-ene (7**).** To a magnetically stirred suspension of methyltriphenylphosphonium iodide (139 mg, 0.342 mmol) in THF (2 mL) was added *n*-BuLi (0.342 mmol) dropwise at 0 °C, which resulted in a yellow coloration. Now, the aldehyde **12** (42 mg, 0.23 mmol), dissolved in THF (2 mL), was added and the resultant mixture stirred for 2 h before it was quenched with saturated aqueous NH₄Cl. The reaction mixture was diluted with Et₂O (5 mL), and the layers were separated. The solvents were removed and the crude product purified by chromatography to give **7** (38 mg, 74% yield). ¹H NMR (400 MHz): δ 1.66–1.76 (m, 1H), 1.79–1.88 (m, 1H), 1.99–2.06 (m, 1H), 2.09–2.15 (m, 3H), 3.09–3.21 (m, 2H), 4.05–4.11 (m, 1H), 4.38–4.43 (m, 1H), 5.02–5.05 (dd, J = 11.0, 1.2 Hz, 1H), 5.40–5.45 (ddd, J = 17.6, 2, 0.7 Hz, 1H), 6.05 (t, J = 3.9 Hz, 1H), 6.37–6.44 (dd, J = 17.6, 11.0 Hz, 1H). ¹³C NMR (50 MHz): δ 20.7, 25.2, 34.6, 38.6, 70.7, 94.0, 113.3, 127.4, 134.6, 138.2. IR (film): 2920, 1610, 1420, 1340, 1260, 1150, 1070, 1050, 900 cm^{−1}. Anal. Calcd for C₁₀H₁₄O₂S: C, 65.90; H, 7.76. Found: C, 65.78; H, 7.63.

General Procedures for Diels–Alder Addition. Method

A. A mixture of one of the dienes **7–9** (0.1 mmol) and a dienophile (0.1 mmol) in dry toluene (5 mL) was either stirred at rt or heated to 110 °C in a sealed tube under N₂. After a given time or completion of the reaction, the solvent was removed, and the crude product was filtered through a short silica gel column. The separation of the isomers was achieved by radial chromatography.

Method B. To a mixture of one of the dienes **7–9** (0.1 mmol) and a dienophile (0.1 mmol) was added 4 M LPNM/1 M LiClO₄/1 M LiBF₄ in acetonitrile (125 μ L). The reaction mixture was stirred under a nitrogen atmosphere at rt or at 0 °C till the completion of the reaction (TLC).

Data for 18a. Mp: 124 °C. ¹H NMR (300 MHz): δ 1.10–1.25 (dq, J = 12.3, 4.0 Hz, 1H), 1.50–1.68 (tq, J = 12.9, 3.6 Hz, 1H), 1.77–1.87 (dt, J = 12.6, 4.2 Hz, 1H), 1.89–2.00 (m, 2H), 2.08 (d, J = 10.8 Hz, 1H), 2.48–2.52 (m, 1H), 2.75–2.88 (m, 2H), 3.00–3.08 (m, 2H), 3.16–3.24 (dt, J = 9.6, 2.4 Hz, 1H), 3.38 (t, J = 8.7 Hz, 1H), 4.06–4.14 (m, 1H), 4.28–4.37 (m, 1H), 5.82 (t, J = 3.9 Hz, 1H), 7.26–7.49 (m, 5H). ¹³C NMR (75 MHz): δ 20.0, 24.7, 29.7, 33.0, 35.4, 37.2, 41.5, 42.5, 70.6, 97.7, 113.0, 126.2, 128.4, 129.1, 131.8, 140.8, 177.4, 178.5. IR (CHCl₃): 3000, 1700, 1200 cm⁻¹. Anal. Calcd for C₂₀H₂₁NO₃S: C, 67.58; H, 5.96. Found: C, 67.45; H, 5.85.

Data for 19a. ¹H NMR (400 MHz): δ 1.50–1.61 (m, 2H), 1.79–1.85 (m, 2H), 1.87–1.95 (m, 2H), 2.18–2.24 (td, J = 12.8, 5.2 Hz, 1H), 2.39–2.46 (m, 1H), 2.84–2.90 (ddd, J = 18.0, 4.8, 2.8 Hz, 1H), 2.95–3.00 (td, J = 10.0, 5.6 Hz, 1H), 3.06–3.12 (td, J = 10.0, 6.0 Hz, 1H), 3.21–3.26 (dt, J = 8.8, 2.8 Hz, 1H), 3.28 (t, J = 8.4 Hz, 1H), 3.89–3.94 (td, J = 9.6, 6.0 Hz, 1H), 4.17 (td, J = 8.8, 5.6 Hz, 1H), 6.16 (t, J = 4 Hz, 1H), 7.28–7.47 (m, 5H). ¹³C NMR (100 MHz): δ 21.6, 22.1, 27.3, 33.0, 34.5, 38.3, 39.6, 42.7, 69.7, 96.5, 120.4, 126.3, 128.4, 129.1, 142.1, 177.2, 178.7. Anal. Calcd for C₂₀H₂₁NO₃S: C, 67.58; H, 5.96. Found: C, 67.44; H, 5.84.

Data for 18b. Mp: 158 °C. ¹H NMR (400 MHz): δ 1.28–1.38 (dq, J = 12.0, 4.0 Hz, 1H), 1.59–1.71 (tq, J = 13.6, 3.7 Hz, 1H), 1.79–1.87 (dt, J = 13.6, 4.12 Hz, 1H), 1.93–1.99 (m, 1H), 2.10–2.13 (d, J = 12.2 Hz, 1H), 2.42–2.45 (m, 1H), 3.09 (s, 3H), 3.04–3.14 (m, 2H), 3.92–3.97 (td, J = 16.1, 2.7 Hz, 1H), 4.17–4.45 (m, 4H), 5.81–5.83 (m, 1H). ¹³C NMR (75 MHz): δ 21.8, 25.0, 30.2, 33.0, 41.7, 42.7, 55.0, 71.5, 95.8, 108.6, 139.7, 152.6, 154.1. IR (CHCl₃): 3000, 1750, 1698, 1640, 1200 cm⁻¹. Anal. Calcd for C₁₃H₁₇N₃O₃S: C, 52.86; H, 5.81; N, 14.24. Found: C, 52.72; H, 5.69.

Data for 19b. Characteristic signals from the ¹H NMR (300 MHz) of a mixture of **18b** and **19b**: δ 2.25–2.37 (m, 1H), 4.60–4.70 (br d, 1H), 6.40 (t, J = 2.4 Hz, 1H).

Data for 18c (Liquid). ¹H NMR (400 MHz): δ 1.17–1.24 (m, 1H), 1.58–1.68 (m, 1H), 1.80–1.87 (dt, J = 12.9, 3.9 Hz, 1H), 1.90–1.96 (m, 2H), 2.10 (d, J = 11.5 Hz, 1H), 2.90–3.18 (m, 4H), 3.19–3.25 (m, 1H), 3.76 (s, 3H), 3.80 (s, 3H), 4.20–4.35 (m, 2H), 5.66 (t, J = 3.4 Hz, 1H). ¹³C NMR (100 MHz): δ 24.7, 27.4, 32.5, 32.7, 39.2, 41.8, 52.2, 71.4, 96.9, 110.7, 129.4, 138.3, 138.8, 167.7, 168.9. Anal. Calcd for C₁₆H₂₀O₅S: C, 59.24; H, 6.22. Found: C, 59.18; H, 6.15.

Data for 19c. Mp: 84 °C. ¹H NMR (400 MHz): δ 1.22–1.30 (dq, J = 12.2, 3.6 Hz, 1H), 1.71–1.76 (m, 1H), 1.80–1.92 (dq, J = 17.1, 4.1 Hz, 2H), 1.92–2.02 (m, 2H), 2.27–2.32 (br d, J = 12.2 Hz, 1H), 2.94–3.20 (m, 4H), 3.44–3.46 (m, 1H), 3.76 (s, 3H), 3.80 (s, 3H), 4.18–4.25 (m, 1H), 6.25 (t, J = 3 Hz, 1H). ¹³C NMR (100 MHz): δ 23.5, 27.7, 32.7, 32.9, 37.7, 41.0, 52.2, 68.7, 97.5, 120.6, 128.7, 137.2, 139.4, 167.6, 169.1. IR (CHCl₃): 2940, 1710, 1420, 1260, 1060 cm⁻¹. Anal. Calcd for C₁₆H₂₀O₅S: C, 59.24; H, 6.22. Found: C, 59.15; H, 6.14.

Data for 18e (R = Me). Mp: 124 °C. ¹H NMR (400 MHz): δ 1.13–1.27 (tq, J = 12.7, 3.6 Hz, 1H), 1.25–1.32 (tt, J = 12.5, 3.6 Hz, 1H), 1.53–1.82 (m, 5H), 1.85–2.08 (m, 2H), 2.10–2.22 (m, 1H), 2.18 (s, 3H), 2.59–2.65 (m, 1H), 2.74–2.81 (m, 1H), 3.01–3.10 (m, 2H), 4.13–4.20 (m, 1H), 4.32–4.38 (m, 1H), 5.69 (d, J = 5.64 Hz, 1H). ¹³C NMR (100 MHz): δ 19.2, 24.1, 25.0, 28.7, 28.8, 32.9, 38.4, 42.7, 51.3, 70.9, 98.0, 115.2, 142.0, 210.7. IR (CHCl₃): 3000, 2940, 1690, 1210 cm⁻¹. Anal. Calcd for C₁₄H₂₀O₂S: C, 66.64; H, 7.99. Found: C, 66.52; H, 7.85.

Data for 18e (R = OEt, Liquid). ¹H NMR (300 MHz): δ 1.20–1.32 (m, 1H), 1.28 (t, J = 7.3 Hz, 3H), 1.39–1.44 (m, 1H), 1.50–2.13 (m, 8H), 2.50–2.60 (m, 1H), 2.68–2.73 (m, 1H), 3.06 (t, J = 5.4 Hz, 2H), 4.09–4.21 (m, 3H), 4.42–4.37 (td, J = 8.7, 5.4 Hz, 1H), 5.67 (br d, J = 5.1 Hz, 1H). IR (film): 2920, 1710, 1440, 1990 cm⁻¹. Anal. Calcd for C₁₅H₂₂O₃S: C, 63.80; H, 7.86. Found: C, 63.65; H, 7.72.

1,4-Dioxo-6-bromospiro[4.5]dec-6-ene (14). A mixture of 2-bromocyclohexenone (2.88 g, 16.4 mmol), ethylene glycol

(2.03 g, 32.8 mmol), and *p*-toluenesulfonic acid (*p*-TSA) (156 mg, 5 mol %) in benzene (200 mL) was refluxed for 12 h under a Dean–Stark setup. The solvent was removed under reduced pressure, and the crude material was chromatographed to furnish **14** (3.10 g, 80%). ¹H NMR (400 MHz): δ 1.77–1.83 (m, 2H), 1.92–1.95 (m, 2H), 2.09–2.13 (m, 2H), 3.98–4.01 (m, 2H), 4.19–4.22 (m, 2H), 6.35 (t, J = 4.2 Hz, 1H). ¹³C NMR (100 MHz): δ 20.3, 27.5, 35.6, 65.8, 105.8, 124.5, 136.1.

1,4-Dioxo-6-formylspiro[4.5]dec-6-ene (15). *n*-BuLi (20 mmol) was added to a THF solution of **14** (4 g, 18.2 mmol) in THF (80 mL) at –80 °C. After 5 min, DMF (1.46 g, 20 mmol) was introduced. The reaction mixture was stirred for 10 min at this temperature, and the cooling bath was removed. The reaction mixture was immediately washed with saturated aqueous NH₄Cl, and the solvent was removed. The residue was purified as quickly as possible by chromatography to obtain **15** (2.75 g, 90%). ¹H NMR (400 MHz): δ 1.80–1.81 (m, 4H), 2.33–2.37 (m, 2H), 3.98–4.07 (m, 2H), 4.20–4.28 (m, 2H), 7.0 (t, J = 3.7 Hz, 1H), 9.46 (s, 1H). ¹³C NMR (100 MHz): δ 19.8, 26.1, 34.4, 65.6, 105.0, 139.9, 153.3, 191.3. Anal. Calcd for C₉H₁₂O₃: C, 64.25; H, 7.20. Found: C, 64.12; H, 7.10.

1,4-Dioxo-6-vinylspiro[4.5]dec-6-ene (16). *n*-BuLi (9.2 mmol) was added dropwise to a magnetically stirred suspension of methyltriphenylphosphonium iodide (3.70 g, 9.15 mmol) in THF (50 mL) at 0 °C. This resulted in a yellow coloration. Now, a solution of the aldehyde **15** (1.28 g, 7.65 mmol) in THF (4 mL) was added dropwise and the reaction mixture stirred for 1 h. The reaction was quenched with saturated aqueous NH₄Cl. The layers were separated, and the organic layer was dried and concentrated. The crude product was purified to **16** (1.12 g, 75%). ¹H NMR (400 MHz): δ 1.70–1.79 (m, 4H), 2.10–2.15 (q, J = 4.9 Hz, 2H), 4.00–4.04 (m, 4H), 5.00–5.03 (dd, J = 11.3, 1.7 Hz, 1H), 5.35–5.41 (dd, J = 17.6, 2.0 Hz, 1H), 6.16 (t, J = 4.2 Hz, 1H), 6.25–6.33 (ddd, J = 18.6, 11.0, 1.0 Hz, 1H). ¹³C NMR (100 MHz): δ 20.2, 25.3, 33.4, 64.7, 106.8, 113.6, 130.4, 133.4, 136.7. Anal. Calcd for C₁₀H₁₄O₂: C, 72.25; H, 8.49. Found: C, 72.13; H, 8.36.

2-Vinyl-2-cyclohexenone (17). A solution of **16** (168 mg, 1 mmol) and *p*-TSA (10 mg, 5 mol %) in acetone (10 mL) was stirred for 1 h at rt. The solvent was removed and the residue purified by chromatography to obtain 100 mg (80%) of **17**. ¹H NMR (400 MHz): δ 1.97–2.04 (quintet, J = 6.8 Hz, 2H), 2.43–2.49 (m, 4H), 5.16 (d, J = 11.2 Hz, 1H), 5.65 (d, J = 17.8 Hz, 1H), 6.50–6.58 (dd, J = 17.6, 11.2 Hz, 1H), 7.04 (t, J = 4.4 Hz, 1H). ¹³C NMR (100 MHz): δ 22.5, 26.1, 38.6, 115.6, 131.1, 136.4, 145.3, 198.4.

3-Methoxy-3-methyl-2-vinylcyclohexene (8). A solution of **17** (124 mg, 1 mmol) in Et₂O (2 mL) was added dropwise to a freshly prepared solution of MeMgI (1.5 mmol) in Et₂O (2 mL) at 0 °C. The reaction mixture was stirred for 30 min and then quenched with saturated aqueous NH₄Cl. The layers were separated, and the solvent was removed. Purification of the crude product afforded 1-methyl-2-vinylcyclohex-2-en-1-ol (126 mg, 90%). ¹H NMR (400 MHz, CDCl₃): δ 1.38 (s, 3H), 1.54–1.80 (m, 4H), 1.83 (br s, 1H), 2.02–2.18 (m, 2H), 5.02–5.05 (dd, J = 11.0, 1.7 Hz, 1H), 5.42–5.47 (dd, J = 17.6, 1.5 Hz, 1H), 5.87 (t, J = 4.2 Hz, 1H), 6.33–6.40 (dd, J = 17.6, 11.2 Hz, 1H). ¹³C NMR (100 MHz): 19.7, 25.9, 27.4, 40.0, 70.2, 114.1, 127.0, 135.5, 141.4.

A solution of the above alcohol (70 mg, 0.5 mmol) in THF (1 mL) was added to a suspension of NaH (29 mg, 0.6 mmol) in THF (2 mL) at 0 °C, and the reaction mixture was stirred for 1 h. MeI (142 mg, 1 mmol) was administered now, and the contents were stirred for 4 h at rt. The reaction mixture was diluted with Et₂O (10 mL), washed with saturated NH₄Cl, and dried, in that order. The solvent was removed and the residue filtered through a short column of silica gel to furnish **8** (65 mg, 85%). ¹H NMR (400 MHz, CDCl₃): δ 1.37 (s, 3H), 1.49–1.54 (m, 1H), 1.55–1.66 (m, 1H), 1.73–1.80 (m, 1H), 1.97–2.03 (dt, J = 12.4, 3.2 Hz, 1H), 2.06–2.12 (m, 2H), 3.13 (s, 3H), 4.97–5.00 (dd, J = 11.0, 1.7 Hz, 1H), 5.50 (dd, J = 17.6, 1.4 Hz, 1H), 6.00 (t, J = 4.2 Hz, 1H), 6.21–6.28 (ddd, J = 17.6, 11.2, 0.8 Hz, 1H). ¹³C NMR (100 MHz): δ 20.5, 25.8, 26.4, 32.7, 49.9, 76.1, 113.5, 129.9, 135.9, 139.6. Anal. Calcd for C₁₀H₁₆O₂: C, 78.89; H, 10.60. Found: C, 78.75; H, 10.45.

3-Methoxy-2-vinylcyclohexene (9). NaBH₄ (38 mg, 1 mmol) was added to a stirred solution of **17** (124 mg, 1 mmol) and CeCl₃·7H₂O (373 mg, 1 mmol) in methanol (2.5 mL) at 0 °C. The reaction mixture was stirred for 20 min, diluted with Et₂O (10 mL), and washed with cold 5% aqueous HCl (3 mL). The aqueous layer was extracted with Et₂O (5 mL), and the combined organic solution was washed with brine (5 mL) and dried. The residue obtained after solvent removal was filtered through a small column of silica gel to obtain 2-vinylcyclohex-2-en-1-ol (100 mg, 80%). ¹H NMR (400 MHz): δ 1.57–1.67 (m, 2H), 1.69–1.80 (m, 1H), 1.88–1.95 (m, 1H), 2.02–2.11 (m, 2H), 2.16–2.22 (m, 1H), 4.47 (s, 1H), 5.02 (dd, J = 11.0, 1.0 Hz, 1H), 5.36 (d, J = 17.8 Hz, 1H), 5.86 (t, J = 3.72 Hz, 1H), 6.26 (dd, J = 17.8, 11.0 Hz, 1H). ¹³C NMR (100 MHz): δ 16.8, 25.8, 30.8, 62.6, 111.4, 132.4, 137.3, 137.8.

The procedure adopted above for the O-methylation of 1-methyl-2-vinylcyclohex-2-en-1-ol was followed to obtain **9** (94%). ¹H NMR (400 MHz): δ 1.43 (tt, J = 13.7, 3.4 Hz, 1H), 1.55–1.60 (m, 1H), 1.67–1.77 (m, 1H), 2.04–2.22 (m, 3H), 3.39 (s, 3H), 3.94 (t, J = 2.9 Hz, 1H), 4.98 (dd, J = 11.0, 0.5 Hz, 1H), 5.21 (d, J = 17.6 Hz, 1H), 5.91 (t, J = 4.16 Hz, 1H), 6.28 (dd, J = 17.6, 10.8 Hz, 1H). ¹³C NMR (100 MHz): δ 17.0, 25.5, 25.9, 56.1, 71.8, 110.9, 133.0, 136.0, 138.2. Anal. Calcd for C₉H₁₄O: C, 78.20; H, 10.22. Found: C, 78.06; H, 10.10.

Data for 20a and 21a (1:1.07). ¹H NMR (400 MHz): δ 1.27 (s, 3H), 1.30 (s, 3H), 1.15–1.60 (m, 4H), 1.76–1.92 (m, 6H), 2.12–2.34 (m, 2H), 2.50–2.55 (m, 2H), 2.79–3.00 (m, 2H), 3.02 (s, 3H), 3.07 (s, 3H), 3.10–3.30 (m, 4H), 5.66 (t, J = 3.7 Hz, 1H), 5.93 (quintet, J = 2 Hz, 1H). ¹³C NMR (100 MHz): δ 20.4, 20.5, 21.6, 21.9, 23.4, 23.7, 25.0, 30.5, 32.4, 34.8, 35.4, 36.9, 39.4, 41.1, 41.9, 43.4, 49.5, 49.9, 76.3, 77.3, 118.4, 120.5, 126.1, 126.2, 128.3, 128.4, 129.0, 129.1, 131.8, 132.0, 142.1, 142.5, 177.1, 178.0, 178.8, 178.9. Anal. Calcd for C₂₀H₂₃NO₃: C, 73.81; H, 7.13. Found: C, 73.66; H, 6.97.

Data for 20b. Characteristic signals of **20b** from the ¹H NMR (400 MHz) spectrum of a mixture of isomers: δ 1.31 (s, 1H), 3.32 (s, 3H), 3.75 (s, 3H), 3.80 (s, 3H), 5.73 (t, J = 3.2 Hz, 1H).

Data for 21b. Characteristic signals of **21b** from the ¹H NMR (400 MHz) spectrum of a mixture of isomers: δ 1.27, (s, 3H), 3.06 (s, 3H), 3.76 (s, 3H), 3.81 (s, 3H), 5.59 (t, J = 2.9 Hz, 1H).

Data for 20b and 21b. ¹³C NMR (100 MHz): δ 21.1, 21.2, 21.8, 22.9, 27.4, 27.5, 33.0, 33.2, 36.3, 37.0, 37.8, 40.5, 49.5, 49.6, 52.2, 75.6, 112.8, 117.1, 128.0, 128.8, 138.5, 138.9, 139.2, 140.0, 167.5, 167.6, 169.4, 169.5.

Data for 22a. Characteristic signals from the ¹H NMR (400 MHz) spectrum of a mixture of isomers (1:4.3): δ 2.00–2.08 (m, 1H), 3.31 (s, 3H), δ 3.53 (m, 1H), 5.72 (t, J = 4.6 Hz, 1H). ¹³C NMR (100 MHz, CDCl₃): δ 20.8, 22.8, 28.4, 33.2, 35.7, 38.1, 41.8, 56.5, 81.4, 116.2, 128.4, 129.1, 131.8, 139.0, 177.4, 178.7.

Data for 23a. Mp: 119 °C. ¹H NMR (400 MHz): δ 1.15–1.25 (dq, J = 12.2, 3.9 Hz, 1H), 1.44–1.53 (tt, J = 12.4, 3.7 Hz, 1H), 1.55–1.65 (m, 2H), 1.75–1.85 (tq, J = 13.2, 1.0 Hz, 1H), 1.94–2.00 (m, 2H), 2.42–2.52 (tdd, J = 18.3, 10.0, 2.4 Hz, 1H), 2.81 (d, J = 18.6 Hz, 1H), 2.90 (t, J = 9.3 Hz, 1H), 3.21 (s, 3H), 3.17–3.35 (m, 2H), 3.79 (t, J = 2.9 Hz, 1H), 5.70 (t, J = 3.0 Hz, 1H), 7.27–7.49 (m, 5H). ¹³C NMR (100 MHz, CDCl₃): δ 20.1, 21.6, 30.5, 31.6, 33.0, 37.7, 41.6, 55.6, 81.8, 119.4, 126.2, 128.5, 129.2, 131.8, 139.0, 177.7, 178.6. Anal. Calcd for C₁₉H₂₁O₃N: C, 73.28; H, 6.80. Found: C, 73.15; H, 6.67.

Data for 22b. Characteristic signals from the ¹H NMR (400 MHz) spectrum of a mixture of isomers: δ 3.42 (s, 3H), 3.77 (s, 3H), 3.79 (s, 3H), 5.62–5.65 (m, 1H).

Data for 23b. Characteristic signals from the ¹H NMR (400 MHz) spectrum of a mixture of isomers: δ 3.19 (s, 3H), 3.76 (s, 3H), 3.80 (s, 3H), 5.58–5.61 (dt, J = 3.2, 1.2 Hz, 1H).

Data for 22c. ¹H NMR (400 MHz): δ 1.12–1.25 (m, 2H), 1.25–1.31 (m, 2H), 1.44 (tq, J = 13.4, 4.3 Hz, 1H), 1.64 (dq, J = 12.4, 5.8 Hz, 1H), 1.73–1.76 (m, 1H), 1.86 (md, J = 13.4 Hz, 1H), 1.97–2.08 (m, 1H), 2.11–2.19 (m, 1H), 2.16 (s, 3H), 2.30–2.35 (m, 1H), 2.74 (ddd, J = 12.6, 5.6, 2.7 Hz, 1H), 3.42 (s, 3H), 3.49–3.52 (m, 1H), 5.62 (br d, J = 5.6 Hz, 1H). ¹³C NMR (100 MHz, CDCl₃): δ 19.5, 24.2, 24.3, 28.7, 29.3, 35.2, 38.7, 51.3, 57.2, 82.3, 115.6, 140.1, 210.9. Anal. Calcd for C₁₃H₂₀O₂: C, 74.95; H, 9.68. Found: C, 74.76; H, 9.54.

Acknowledgment. We thank the CSIR, Government of India, for financial support and the staff of the Computer Center, Indian Institute of Technology, Kanpur, for generous allocation of computer time on the Silicon Graphics series of minisupercomputers.

Supporting Information Available: Copies of the ¹H and ¹³C spectra of several of the compounds, Cartesian coordinates of the optimized structures of **7a** and **7b** and their Li⁺ complexes, and ORTEP plots of the X-ray crystal structures of **18a**, **19a**, **18b**, **18e**, **19c**, and **23a**. This material is available free of charge via the Internet at <http://pubs.acs.org>.

JO0106400